

**The structure and evolution of weakly self-interacting cold dark  
matter halos**

Andreas Burkert

Max-Planck-Institut für Astronomie, Königstuhl 17,

D-69117 Heidelberg,

Germany

Received \_\_\_\_\_; accepted \_\_\_\_\_

## ABSTRACT

The evolution of halos consisting of weakly self-interacting dark matter particles is investigated using a new numerical Monte-Carlo N-body method. The halos initially contain kinematically cold, dense  $r^{-1}$ -power-law cores. For interaction cross sections  $\sigma^* = \sigma/m_p \geq 10 - 100 \text{ cm}^2 \text{ g}^{-1}$  weak self-interaction leads to the formation of isothermal, constant density cores within a Hubble time as a result of heat transfer into the cold inner regions. This core structure is in good agreement with the observations of dark matter rotation curves in dwarf galaxies. The isothermal core radii and core densities are a function of the halo scale radii and scale masses which depend on the cosmological model. Adopting the currently popular  $\Lambda$ CDM model, the predicted core radii and core densities are in good agreement with the observations. For large interaction cross sections, massive dark halos with scale radii  $r_s \geq 1.4 \times 10^4 (\text{cm}^2 \text{ g}^{-1} / \sigma^*)$  kpc could experience core collapse during their lifetime, leading to cores with singular isothermal density profiles.

*Subject headings:* dark matter – galaxies: halos – galaxies: formation – galaxies: kinematics and dynamics – methods: numerical

## 1. Introduction

Cosmological models with a dominant cold dark matter component predict dark matter halos with strongly bound, kinematically cold cores (Dubinski & Carlberg 1991, Warren *et al.* 1992, Navarro *et al.* 1997). Within the core region, the dark matter density increases as a power-law  $\rho \sim r^{-\gamma}$  with  $\gamma$  in the range of 1 to 2 and the velocity dispersion  $\sigma$  decreases towards the center (Carlberg 1994, Fukushige & Makino 1997). Numerous numerical simulations (e.g. Moore *et al.* 1998, Huss *et al.* 1999, Jing & Suto 2000), as well as analytical theory (Syer & White 1998, Kull 1999), have shown that such a core structure follows naturally from collisionless hierarchical merging of cold dark matter halos, independent of the adopted cosmological parameters.

It has recently become clear that on galactic scales the predictions of cold dark matter models are not in agreement with several observations. High-resolution calculations by Klypin *et al.* (1999) and Moore *et al.* (1999) have shown that the predicted number and mass distribution of galaxies in galactic clusters is consistent with the observations. However, on scales of the Local Group, roughly one thousand dark matter halos should exist as separate, self-gravitating objects, whereas less than one hundred galaxies are observed. This disagreement can be attributed to the high core densities of satellite dark halos in cosmological models which stabilize them against tidal disruption on galactic scales. Mo *et al.* (1998) and lateron Navarro and Steinmetz (2000) found that cold-dark matter models reproduce well the I-band Tully-Fisher slope and scatter. They however fail to match the zero-point of the Tully-Fisher relation as well as the relation between disk rotation speed and angular momentum. Again, this problem can be traced to the excessive central concentrations of cold dark halos. Finally, recent observations of dark matter dominated rotation curves of dwarf galaxies have indicated shallow dark matter cores which can be described by isothermal spheres with finite central densities (Moore 1994, Flores & Primack

1994, Burkert 1995, de Blok & Mc Gaugh 1997, Burkert & Silk 1999, Dalcanton & Bernstein 2000, see however van den Bosch *et al.* 1999), in contrast to the power-law cusps, expected from cosmological models. The disagreement between observations and theory indicates that a substantial revision to the cold dark matter scenario might be required which could provide valuable insight into the origin and nature of dark matter.

Motivated by these problems, Spergel & Steinhardt (1999) proposed a model where dark matter particles experience weak self-interaction on scales of kpc to Mpc for typical galactic densities. They noted that self-interaction could lead to satellite evaporation due to the dark particles within the satellites being kicked out by high-velocity encounters with dark particles from the surrounding dark halo of the parent galaxy. In order for weak interaction to be important on galactic scales, they estimate that the ratio of the collision cross section and the particle mass should be of order  $\sigma_{wsi}/m_p \approx 1 \text{ cm}^2 \text{ g}^{-1}$ .

The Spergel and Steinhardt model has already motivated several follow-up studies. For example, Ostriker (1999) demonstrated that weak self-interaction would have the interesting side product of naturally growing black holes with masses in the range  $10^6 - 10^9 M_\odot$  in galactic centers. Hogan & Dalcanton (2000) investigated analytically the effect of particle self-interactions on the structure and stability of galaxy halos. Moore et al. (2000), adopting a gas-dynamical approach, showed that in the limit of infinitely large interaction cross sections dark halos would develop singular isothermal density profiles which are not in agreement with observations. Mo & Mao (2000) and Firmani et al. (2000) investigated the affect of self-interaction on rotation curves. In addition, models of repulsive dark matter (Goodman 2000), fluid dark matter (Peebles 2000) and self-interacting warm dark matter (Hannestad & Scherrer 2000) have recently been discussed.

In this paper we will investigate the effect of weak self-interaction on the internal structure of cold dark matter halos. If the interaction cross section is not exceptionally

large, the dark matter system cannot be treated as a collision dominated, hydrodynamical fluid. Section 2 therefore introduces a new numerical Monte-Carlo-N-body (MCN) method for weakly interacting particle systems. Initial conditions are discussed in section 3. Using the MCN-method, the evolution of weakly self-interacting dark matter halos is investigated in section 4. Conclusions follow in section 5.

## 2. The Monte-Carlo N-body method

Within the framework of weak self-interacting, the mean free path  $\lambda$  of a dark matter particle is determined by  $\lambda = (\rho\sigma^*)^{-1}$ , where  $\rho$  is the local dark matter mass density and  $\sigma^* = \sigma_{wsi}/m_p$  is the ratio between the self-interaction collision cross section  $\sigma_{wsi}$  and the particle mass  $m_p$ . If, within a timestep  $\Delta t$ , the path length  $l = v\Delta t$  of a particle with velocity  $v$  is short compared to  $\lambda$ , the probability  $P$  for it to interact with another particle can be approximated by

$$P = l/\lambda = \sigma^* \rho v \Delta t. \tag{1}$$

We use a Monte-Carlo approach in order to include weak self-interaction in a collisionless N-body code that utilizes the special purpose hardware GRAPE (GRAvity PipE; Sugimoto et al. 1990) in order to determine the gravitational forces between the dark matter particles by direct summation. For each particle, a list of its 50 nearest neighbors is returned by the boards which allows the determination of the local dark matter mass density  $\rho$ . The particle experiences an interaction with its nearest neighbor with a probability given by equation (1). Each weak interaction changes the velocities of the two interacting particles. Here, due to the lack of a more sophisticated theory, we assume that the interaction cross section is isotropic and that the interaction is completely elastic. In

this case, the directions of the velocity vectors after the interaction are randomly chosen and their absolute values are completely determined by the requirement of energy and momentum conservation.

The computational timestep  $\Delta t$  must be chosen small enough in order to guarantee that the evolution is independent of the numerical parameters, that is the adopted timestep and the number of particles. Otherwise, particles with large velocities could penetrate too deeply into a dense region like the core of a dark matter halo, violating the requirement  $l \ll \lambda$ . Test calculations have shown that  $\Delta t \leq \eta(\sigma^* \rho v)^{-1}$  with  $\eta \approx 0.1$  leads to reliable results that are independent of the numerical parameters.

### 3. Initial conditions

Cold dark matter halos form on dynamical timescales. If  $\sigma^*$  is small enough, the halos will achieve an equilibrium state within a few dynamical timescales that is determined by collisionless dynamics alone, before self-interaction becomes important. The structure of the halos subsequently changes due to self-interaction on longer timescales. This secular evolution is similar to the long-term evolution of globular clusters which experience core collapse due to gravitational 2-body encounters after virialization.

We start with an equilibrium model of a virialized dark matter halo and study its secular dynamical evolution due to weak self-interaction using the MCN-method. As initial condition, a Hernquist halo model (Hernquist 1990) is adopted. Its density distribution is  $\rho(r) = \rho_s / (r/r_s(1 + r/r_s)^3)$  where  $\rho_s$  and  $r_s$  are the scale density and scale radius, respectively. The mass profile is  $M(r) = Mr^2 / (r_s + r)^2$  with  $M$  the finite total halo mass. Assuming hydrostatic equilibrium and an isotropic velocity distribution, the velocity dispersion is zero at the center and increases outwards, reaching a maximum at the

inversion radius  $r_i = 0.33r_s$  outside of which it decreases again. A similar structure is seen in cosmological simulations (Carlberg 1994, Fukushige & Makino 1997). In general, within the interesting region  $r \leq r_s$  the Hernquist model provides an excellent fit to the structure of cold dark matter halos that result from high-resolution cosmological models. Only in the outermost regions do the dark matter halo profiles deviate significantly from the Hernquist model, predicting a density distribution that decreases as  $r^{-3}$  and a dark halo mass that diverges logarithmically (Navarro *et al.* 1997). Note, that our model neglects any clumpy substructure that might exist within dark matter halos (Moore *et al.* 1999). This should be a reasonable approximation for the inner regions where satellites are efficiently disrupted by tidal forces. The evolution of weakly self-interacting, clumpy dark halos will be presented in a subsequent paper (see also Moore *et al.* 2000).

In the following, we will adopt dimensionless units:  $G=1$ ,  $r_s = 1$  and  $M = 1$ . The total mass and the mean mass density within the inversion radius  $r_i$  is  $M_i = 0.06$  and  $\rho_i = 0.4$ , respectively, leading to a dynamical timescale within  $r_i$  of  $\tau_{dyn} = 0.8$ . Most numerical calculations have been performed adopting 80000 particles and a gravitational softening length of  $\epsilon = 0.002 \times r_s$ . Test calculations with 120000 particles did not change the results. N-body calculations without weak interaction have shown that the dark halo is stable and its density distribution does not change outside of  $r \geq 0.006 \times r_s$  within 20 dynamical timescales.

#### 4. The evolution of weakly self-interacting dark halos

Figure 1 shows the evolution of the dark matter density distribution and the velocity dispersion profile inside the core region, adopting a collision cross section  $\sigma^* = 10 \times r_s^2 / M_s$ . The density distribution initially has the characteristic power-law cusp and the velocity dispersion decreases towards the center for  $r < r_i$ . Within this region, the kinetic

temperature inversion leads to heat conduction inwards. The central velocity dispersion increases with time and the core expands, resulting in a shallower density distribution. After 3 dynamical timescales, an isothermal, constant density core has formed with a radius that is of order the initial inversion radius  $r_i$ . Subsequently, weak interactions between the kinematically hotter core and the cooler envelope lead to a flow of kinetic energy outwards which causes the isothermal core to contract and heat up further due to its negative specific heat, starting a core collapse phase. The calculations are stopped after 16 dynamical timescales when the central density and the central velocity dispersion has increased further by a factor of 4 and 1.4, respectively. Note that during the core collapse phase, the system maintains an isothermal, constant density core with the core radius decreasing with time. Overall, the evolution of the dark halo is very similar to the secular evolution of particle systems with Hernquist profiles that are affected by gravitational 2-body interactions (Heggie *et al.* 1994, Quinlan 1999).

Several calculations with different interaction cross sections  $\sigma^*$  have been performed. In all cases, the evolution is similar to that shown in Fig. 1, independent of the adopted collision cross section. The timescale  $\tau_{iso}$  for the formation of the isothermal constant density core does however depend on  $\sigma^*$  with

$$\tau_{iso} \approx \frac{30\tau_{dyn}}{\sigma^*} \frac{r_s^2}{M_s}. \quad (2)$$

In agreement with the calculations of Quinlan (1999) the core collapse timescales are roughly an order of magnitude larger than  $\tau_{iso}$ .

Observations of dark matter dominated dwarf galaxies show a characteristic dark matter core structure that can be fitted well by the empirical density distribution (Burkert 1995)  $\rho = \rho_0 * (r + r_0)^{-1}(r^2 + r_0^2)^{-1}$  where  $\rho_0$  and  $r_0$  are the isothermal core density and radius, respectively. Figure 2 compares this profile (solid line) with the core structure of

weakly interacting dark halos at  $t = 0$  (dashed line) and after core expansion at  $t = \tau_{iso}$  (points with error bars). It is well known that power-law cores do not provide a good fit to the observations. An excellent agreement can however be achieved after core expansion if one adopts the following core parameters

$$\begin{aligned} r_0 &\approx 0.6r_i \\ \rho_0 &\approx 1.54M_i r_i^{-3} \end{aligned} \tag{3}$$

where  $M_i$  is the initial dark matter mass inside the inversion radius  $r_i$ .

## 5. Conclusions

The previous MCN calculations have shown that isothermal cores with shallow density profiles form naturally in weakly interacting dark halos. The cores have density distributions that are in excellent agreement with the observations of dark matter rotation curves in dwarf galaxies. The core size is determined by the radius  $r_i$  inside which heat is conducted inwards, that is where the initial velocity dispersion decreases towards the center. Note, that this conclusion should be valid, independent of whether the density diverges as  $\rho \sim r^{-1}$  or even steeper (Moore *et al.* 1998, Jing & Suto 2000) for  $r \ll r_s$ .

A quantitative comparison with the observations requires the determination of the typical scale parameters  $r_s$  and  $M_s$  for dark matter halos. Recent cosmological  $\Lambda$ CDM models (Navarro & Steinmetz 2000) predict that cold dark matter halos with total masses  $M_{200} \approx 10^{10} - 10^{12} M_\odot$  should have concentrations  $c = r_{200}/r_s \approx 20$ , where  $M_{200}$  is the total dark matter mass within the virial radius  $r_{200}$  which denotes the radius inside which the averaged overdensity of dark matter is 200 times the critical density of the universe. Adopting a Hubble constant  $h=0.7$  leads to  $r_{200} = 0.02 (M_{200}/M_\odot)^{1/3}$  kpc  $\approx 40 - 200$  kpc

and with  $c=20$  to scale radii  $r_s \approx 2 - 10$  kpc. For a NFW-profile (Navarro *et al.* 1997) the dark matter mass inside  $r_s$  is  $M_s \approx 0.1 M_{200}$  and the core density is  $M_s/r_s^3 \approx 0.01 M_\odot \text{ pc}^{-3}$ . In contrast to the Hernquist model with  $r_i = 0.33r_s$ , the inversion radius of the NFW-profiles coincides with the scale radius  $r_i = r_s$  due to the shallower outer density distribution. According to equation 3, weak interaction in NFW-halos should therefore lead to isothermal cores with radii  $r_0 \approx 0.6 r_s \approx 1.2 - 6$  kpc and densities  $\rho_0 \approx 1.55 M_s r_s^{-3} \approx 1.5 \times 10^{-2} M_\odot \text{ pc}^{-3}$ . The observations indicate core radii  $r_0 \approx 2 - 10$  kpc with core densities  $\rho_0 \approx 0.01 M_\odot \text{ pc}^{-3}$  (Burkert 1995), in very good agreement with the theoretical predictions.

In order for dark matter cores to be affected by weak self-interaction, the core expansion timescale must be smaller than the age  $\tau$  of the halo:  $\tau_{iso} \leq \tau \approx 100\tau_{dyn}$ . With equation (2) and adopting  $M_s/r_s^3 \approx 0.01M_\odot \text{ pc}^{-3}$ , this requirement leads to a minimum value of the collision cross section for weak self-interaction to be important

$$\sigma^* \geq 100 \left( \frac{kpc}{r_s} \right) \left( \frac{cm^2}{g} \right) \quad (4)$$

Note, that this lower limit would be a factor of 25 larger if cosmological models underestimate the scale radii of dark halos by a factor of 5.

Dark matter halos with  $\tau_{iso} \approx \tau_{dyn}$  are likely to have gone through core collapse if their ages are  $\tau \gg \tau_{dyn}$ . This condition requires the halo core radii to be larger than  $r_s > 1.4 \times 10^4 (cm^2 g^{-1})/\sigma^* \text{ kpc}$ , indicating that more massive halos could have experienced core collapse while lower mass halos could still be in the process of core expansion.

I would like to thank Matthew Bate for providing a subroutine to find nearest neighbors using GRAPE and Paul Steinhardt, Ben Moore and Jerry Ostriker for interesting discussions and the referee for important comments. Special thanks to David Spergel for

pointing out the different dependence of the inversion radius on the scale radius for NFW- and Hernquist profiles.

## REFERENCES

- Burkert, A. 1995, *ApJ*, 447, L25.
- Burkert, A. & Silk 1997, *ApJ*, 488, L55.
- De Blok, W.J.G. & McGaugh, S.S. 1997, *MNRAS*, 290, 533.
- Carlberg, R. 1994, *ApJ*, 433, 468.
- Dalcanton, J.J. & Bernstein, R.A. 2000, *ASP Conference Series*, 197, 161.
- Dubinski, J. & Carlberg, R. 1991, *ApJ*, 378, 496.
- Firmani, C., D’Onghia, E., Avila-Reese, V., Chincarini, G. & Hernández, X. 2000, [astro-ph/0002376](#).
- Flores, R.A. & Primack, J.R. 1994, *ApJ*, 427, L1.
- Fukushige, T. & Makino, J. 1997, *ApJ*, 477, L9.
- Goodman, J. 2000, [astro-ph/0003018](#).
- Heggie, D.C., Inagaki, S. & McMillan, S.L.W. 1994, *MNRAS*, 271, 706.
- Hernquist, L. 1990, *ApJ*, 356, 359.
- Hogan, C.J. & Dalcanton, J.J. 2000, [astro-ph/0002330](#).
- Huss, A., Jain, B. & Steinmetz, M. 1999, *ApJ*, 517, 64.
- Jing, Y.P. & Suto, Y. 2000, *ApJ*, 529, L69.
- Klypin, A., Kravtsov, A.V., Valenzuela, O. & Prada, F. 1999, *ApJ*, 522, 82.
- Kull, A. 1999, *ApJ*, 516, L5.
- Mo, H.J., Mao, S. & White, S.D.M. 1998, *MNRAS*, 295, 319.
- Mo, H.J. & Mao, S. 2000, [astro-ph/0002451](#).
- Moore, B. 1994, *Nature*, 370, 629.

- Moore, B., Governato, F., Quinn, T., Stadel, J. & Lake, G. 1998, *ApJ*, 499, L5.
- Moore, B., Ghigna, S., Governato, F., Lake, G., Quinn, T. & Stadel, J. 1999, *ApJ*, 524, L19.
- Moore, B., Gelato, S., Jenkins, A., Pearce, F.R. & Quilis, V. 2000, *astro-ph/0002308*.
- Navarro, J.F., Frenk, C.S. & White, S.D.M. 1997, *ApJ*, 490, 493.
- Navarro, J.F. & Steinmetz, M. 2000, *astro-ph/0001003*.
- Ostriker, J.P. 1999, *astro-ph/9912548*.
- Peebles, P.J.E. 2000, *astro-ph/0002495*.
- Quinlan, G. 1999, *astro-ph/9606182*.
- Spergel, D.N. & Steinhardt, P.J. 1999, *astro-ph/9909386*.
- Sugimoto, D., Chikada, Y., Makino, J., Ito, T., Ebisuzaki, T. & Umemura, M. 1990, *Nature*, 345, 33.
- Syer, D. & White, S.D.M. 1998, *MNRAS*, 293, 337.
- van den Bosch, F.C., Robertson, B.E., Dalcanton, J.J. & de Blok, W.J.G. 1999, *astro-ph/9911372*
- Warren, S.W., Quinn, P.J., Salmon, J.K. & Zurek, H.W. 1992, *ApJ*, 399, 405.

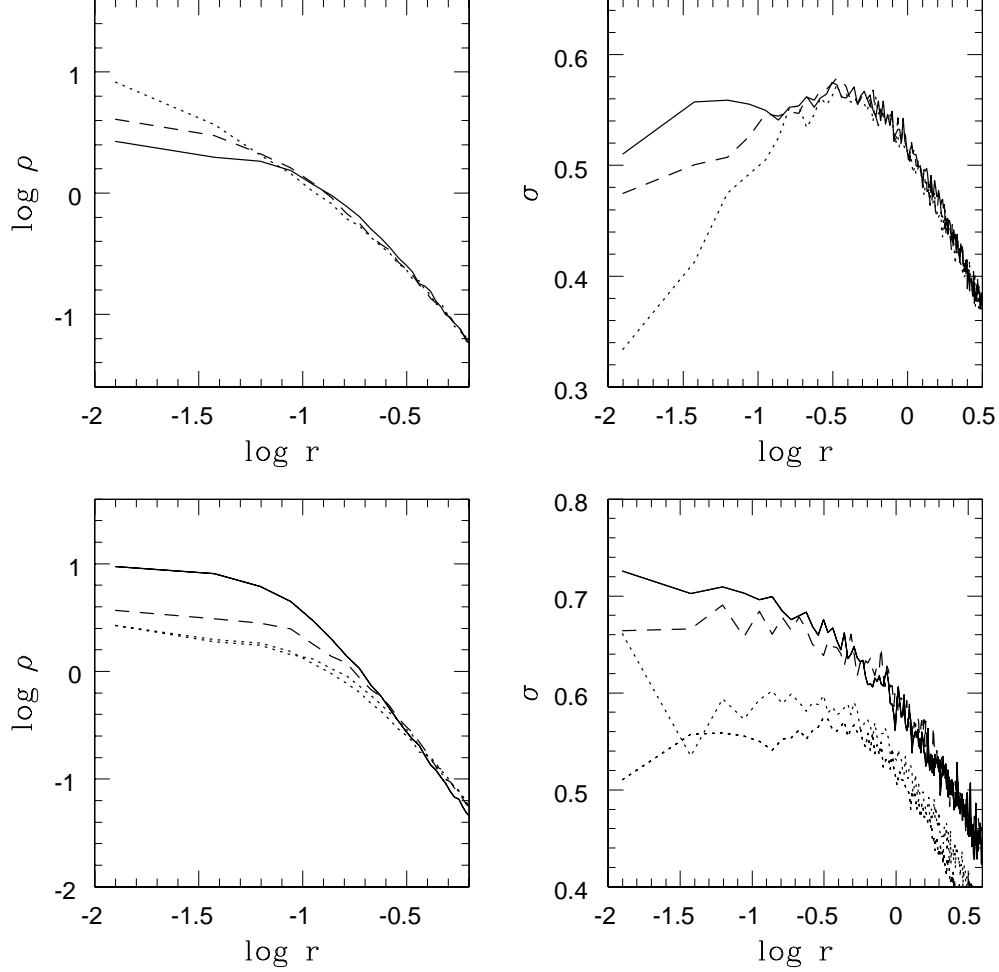


Fig. 1.— Figure 1: The evolution of the dark matter density distribution  $\rho(r)$  and of the 3-dimensional velocity dispersion profile  $\sigma(r)$  in dimensionless units is shown, adopting a weak interaction cross section of  $\sigma^* = 10 r_s^2/M_s$ . The upper panels show the phase of core expansion with the dotted curves representing the initial conditions and the dashed and solid curves corresponding to the evolutionary state of  $t=1 \tau_{dyn}$  and  $t=2.5 \tau_{dyn}$ , respectively. The lower panels show the epoch after core expansion (lower dotted lines:  $t=2.5 \tau_{dyn}$ , upper dotted lines:  $t=5 \tau_{dyn}$ ) and the subsequent phase of core collapse (dashed line:  $t=10\tau_{dyn}$ , solid line:  $t=16 \tau_{dyn}$ ).

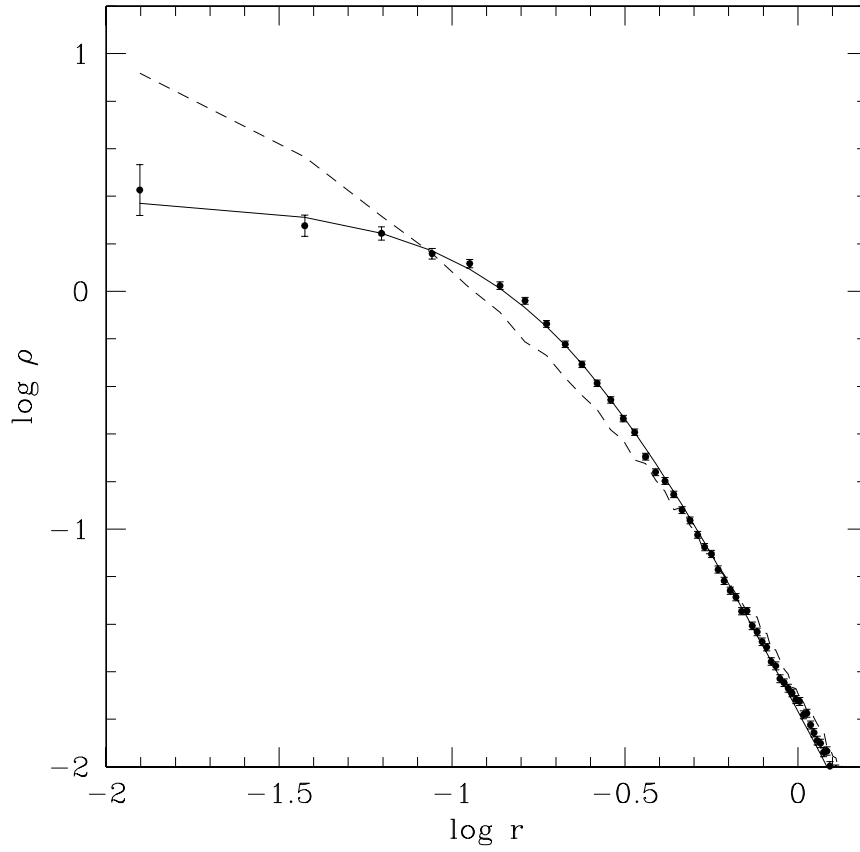


Fig. 2.— Figure 2: The dark matter density distribution as inferred from rotation curves of dwarf galaxies (solid line) is compared with halo density distribution at  $t=0$  (dashed line) and after core expansion at  $t = \tau_{iso}$ .